

Article

Drift Velocity with Elastic Scattering

Rachel M. Morin *  and Nicholas A. Mecholsky 

Department of Physics and Vitreous State Laboratory, The Catholic University of America, Washington, DC 20064, USA; nmech@vsl.cua.edu

* Correspondence: morinrm@cua.edu

Abstract: The drift velocity of a particle under a driving force has its roots in the theory of electrical conduction. Although it has been studied for over 100 years, it still yields surprises. At the heart of a particle's drift velocity is an interplay of classical, quantum, and statistical mechanics. Irreversibility and energy loss have been assumed as essential features of drift velocities and very little effort has been made to isolate the aspects of particle transport that are due to elastic mechanisms alone. In this paper, we remove energy loss and quantum mechanics to investigate the classical and statistical factors that can produce a drift velocity using only elastic scattering. A Monte Carlo simulation is used to model a particle in a uniform force field, subject to randomly placed scatterers. Time-, space-, and energy-dependent scattering models, with varied ranges of scattering angles, are investigated. A constant drift velocity is achieved with the time scattering model, which has a constant average time between scattering events. A decreasing drift velocity is observed for space and energy-dependent models. The arrival of a constant drift velocity has to do with a balance of momentum gained between collisions and momentum lost after a collision.

Keywords: scattering; charge transport; drift velocity; Monte Carlo; elastic

MSC: 60G50



Citation: Morin, R.M.; Mecholsky, N.A. Drift Velocity with Elastic Scattering. *Axioms* **2023**, *12*, 1076. <https://doi.org/10.3390/axioms12121076>

Academic Editors: Francesco dell'Isola, Hovik Matevosian and Giorgio Nardo

Received: 1 October 2023

Revised: 11 November 2023

Accepted: 16 November 2023

Published: 24 November 2023



Copyright: © 2023 by the authors. Licensee MDPI, Basel, Switzerland. This article is an open access article distributed under the terms and conditions of the Creative Commons Attribution (CC BY) license (<https://creativecommons.org/licenses/by/4.0/>).

1. Introduction

The drift velocity of a semiconductor or metal is an experimentally measurable quantity which is directly related to the transport properties of the material, such as its conductivity or mobility. If the drift velocity of a material can be predicted based on its properties, then we can design more efficient high speed and lower power consuming devices, such as solar cells [1], small devices [2] and two-dimensional materials [3]. From Drude to Sommerfeld and beyond, many theories have been formulated to explain why electrons or other charge carriers arrive at a constant drift velocity in materials. All drift velocity theories include some form of scattering mechanism in order to counterbalance the applied electric field and maintain the electrons at thermal equilibrium with the material [4–7]. However, as these mechanisms have been identified and studied (phonons, impurities, other carriers, etc.) [8], many mechanisms are implemented in an elastic way [9,10]. In fact, as scattering models are refined, they are often done so in an elastic way, pushing inelasticity into other ill-defined parts of the model. We could go further and claim that inelasticity in a classical or quantum model is a measure of ignorance of physical mechanisms rather than pure irreversibility which must be its ultimate origin.

This study investigates the possibility of achieving a constant drift velocity with only elastic scatterers. The drift velocity phenomena is a common statistic across many applications. Monte Carlo methods in general, as in refs. [11–17], deal with similar collision mechanisms and could benefit from a systematic study of how the drift velocity develops in the collective motions of particles. In our experience, we are motivated specifically by transport in semiconductors. In a classical paper on charge transport in semiconductors by Jacoboni and Reggiani, as well as in other sources [4,9], we find many quantum mechanical

elastic and inelastic scattering mechanisms that may or may not lead to constant drift velocities during Monte Carlo simulations. However, in the much simpler Drude model, a constant drift velocity develops, but with less accurate physical modeling of the scattering mechanism. In order to prepare to investigate the possibility of achieving a constant drift velocity with elastic scattering, we will briefly review the Drude model assumptions and indicate how the drift velocity develops. Next, we will summarize different semiclassical scattering mechanisms as motivation for focusing on elastic scattering as a possible independent mechanism for providing a zero or constant drift velocity. Finally, simple models are proposed to determine which parameters will produce a constant drift velocity with only elastic scattering.

The classical model proposed by Drude makes several assumptions: (1) the electrons have a relaxation time τ and the probability of scattering within a time interval dt is dt/τ , which is taken to be independent of the electrons' position and velocity, (2) once a scattering event occurs, the electron's momentum resets to a value related to the temperature of the material—the electron is assumed to achieve thermal equilibrium with its surroundings only through collisions—and (3) in between scattering events, the electrons respond to external electric and magnetic fields, but otherwise have no other interactions with their surroundings [4,5].

According to the Drude model, the arrival of a constant drift velocity is therefore explained by a simple process where the electrons in a material, on average, only gain as much energy as the electric field supplies in time between scattering events. The momentum reset means that the electrons, after scattering, on average lose all energy gained since the last scattering event and therefore all memory of past scattering events. In the Sommerfeld model, the drift velocity corresponds to a net shift in momentum of all the electrons, defined by the Fermi surface. When an electric field is applied to the material, the net momentum will shift at a constant rate. Scattering with a relaxation time, τ , is again necessary in order to counterbalance the electric field and arrive at a constant drift velocity, where the momentum reaches a final net displacement [6]. The relaxation time corresponds to the time during which the field acts on the carrier, and it also assumes a momentum reset after each collision.

A semi-classical model combines quantum mechanics with the Sommerfeld and Drude models. It treats the electrons or charge carriers as classical quasiparticles, tracking their momenta and position ballistically [4]. The non-classical behavior is introduced in the scattering mechanisms. Jacoboni and Reggiani [9] outline a Monte Carlo method that utilizes this semi-classical model. The program tracks the motion of the electron and determines when it will scatter based on the relative probabilities of the different scattering events in a given material. The elastic or inelastic behavior of each scattering mechanism is encoded into the equations which approximate the change in momentum of the electron after scattering.

The scattering mechanisms in metals and semiconductors have been studied, and are still being unraveled. These include acoustic and optical phonon, ionized impurity, impact ionization, and carrier–carrier scattering [9]. Of these scattering mechanisms, phonon scattering is sometimes elastic and ionized impurity scattering is always elastic, and at sufficiently low temperatures, elastic ionized impurity scattering will dominate [4].

The ideal elastic scattering mechanism would result in the electron keeping its kinetic energy after scattering. This study utilizes the semi-classical Monte Carlo method proposed by Jacoboni and Reggiani, replacing the scattering mechanisms and probabilities of scattering with simplified models. Of the different models investigated, only a model with a constant time between scattering events will result in a constant drift velocity. Other models include a space-dependent model, which keeps a constant distance between collisions, and an energy-dependent model, where the rate of scattering is proportional to the kinetic energy of the electron. For these latter models, a constant drift velocity is not achieved. In fact, the average velocity in the direction of the applied field slows down and approaches zero.

This paper attempts to provide a few simple models using elastic scattering that can provide various drift velocities. The main conclusion is that, in a variety of abstracted situations, the assumed key ingredient of inelasticity in scattering is not necessary to provide a constant drift velocity. We focused on models that are inspired by electron scattering in semiconductors, but are not encumbered by the complications necessary to approach a physical reality to show that the details of the elastic scattering mechanism itself (independent of inelastic processes) can lead to zero or non-zero drift velocities.

2. Methods

In order to investigate whether a constant drift velocity could be achieved with only elastic scattering mechanisms, a simple semi-classical model was developed. The model consists of a point particle accelerated by a uniform force field subject to random elastic scattering mechanisms (scatterers). Here, we are generalizing the “electron” in traditional drift velocity calculations to be any “particle” in an equivalent system. Elastic scattering was implemented by assuming the particle lost no kinetic energy during a scattering event. The acceleration \vec{a} due to the force field \vec{F} was assumed to be constant. By analogy, the particle could be thought of as a projectile falling in a uniform gravitational field, elastically colliding with random stationary scatterers at a certain rate. The scattering rate was determined by three different methods in order to pinpoint the parameters that produce a constant drift velocity. The first method, called time-dependent scattering (TDS), chooses a random time between each collision. The second method, space-dependent scattering (SDS), chooses a random distance between collisions. The third method, energy-dependent scattering (EDS), where scattering rate is dependent on the kinetic energy of the particle, chooses the time between scattering events based on the velocity of the particle. Only 2D models are discussed. This is because three-dimensional versions of the models have been observed not to affect the drift velocity measurements in the case of elastic scattering.

2.1. Monte Carlo Program Outline

The structure of the program is similar to a random walk, where the position and velocity of the particle are continually evaluated and updated. It is outlined as follows:

1. We begin with a single particle with initial conditions of motion (position and velocity).
2. At every collision, the program determines (1) the time of flight before the next scattering event using one of the three methods above, TDS, SDS, or EDS, and (2) the scattering angle.
3. The final position of the particle after scattering, its velocity after scattering, the time of flight, and total running simulation time are recorded.
4. A single run will evolve a particle from its initial conditions for a given number of steps.

For statistically significant results, each program was evaluated for as many steps as was needed to see the general trend of the particles’ motion, and repeated for enough runs to get a smooth result upon averaging.

2.2. Models

Three different types of models are used to find the time between scattering events: time-dependent, space-dependent, and energy-dependent scattering. Within the time-dependent scattering model, different ranges of scattering angles are also tested (vertical exclusion angle, symmetric exclusion angle, and directional exclusion angle). The acceleration due to the external force for all models is set at $\vec{a} = -10 \text{ m} \times \text{s}^{-2} \hat{y}$. The units meters (m) and seconds (s) are chosen arbitrarily and can be scaled without affecting the overall trend of the results.

2.2.1. Time-Dependent Scattering (TDS)

In the time-dependent scattering (TDS) method, there are two random variables: the time between collisions (scattering time) t and the scattering angle after collision θ . The time between collisions was chosen to be either a constant (0.5 s), a random variate from

an exponential distribution with a relaxation time of $\tau = 1$ s, or a random variate from a uniform distribution between 0–1 s. All distributions have the same average time between scattering events: 0.5 s. In order to model varying angular dependencies on scattering rates that would occur in hard-sphere and other physical collisions, four basic types of scattering angle distributions were investigated:

- (a) A uniform distribution between $0-2\pi$.
- (b) A vertical exclusion angle, which omitted a range of scattering angles in the $-y$ direction.
- (c) A symmetric exclusion angle, which excluded scattering angles in the positive and negative y directions for a given range. This type of distribution does not allow scattering in the direction of the force, nor in the opposite direction.
- (d) A directional exclusion angle, which omitted a range of scattering angles in the direction of the particle’s travel. This is most similar to hard-sphere scattering.

See Figure 1.

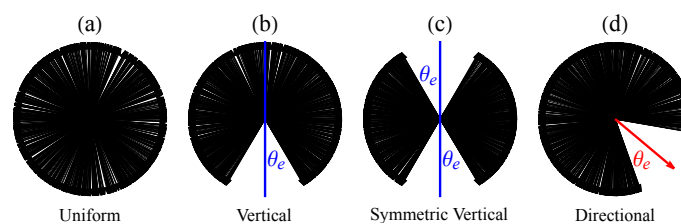


Figure 1. Four different models for exclusion angles. The half-angle θ_e is the exclusion angle. The black arrows represent allowed scattering angles for each model. (a) The uniform distribution of angles allows all scattering angles between $0-2\pi$. (b) The vertical exclusion angle excludes the particle from scattering in the direction of the force for a range given by the half angle θ_e . (c) The symmetric vertical exclusion angle disallows scattering both in the direction of the force and in the opposite direction for the same range. (d) The directional exclusion angle disallows scattering in the direction of the particle’s motion just before a scattering event. The red arrow represents the direction of motion before scattering.

2.2.2. Space-Dependent Scattering (SDS)

In the space-dependent scattering (SDS) method, the random variables are the distance between scattering events and the scattering angle. The distance between collisions was chosen to be either constant, a random variate from an exponential distribution, or a random variate from a distribution of “nearest neighbors”. The nearest neighbor distribution (NND) is the distribution of radial distances r from a given random point to its nearest neighbor in a 2D random field of points. The NND was found both empirically by plotting a set of random points and plotting a histogram of the distances between nearest neighbors in the set and analytically using the assumptions of a Poisson point process [18]. The probability distribution function of the NND is given by:

$$NND_{2D}(r) = 2\pi\rho r e^{-\rho\pi r^2} \tag{1}$$

where r is the radial distance, and the range of the distribution is $[0, \infty)$. The NND is directly related to the number density ρ of scatterers. After the distance was determined, then the time to the next collision was calculated using the usual kinematic equations.

The exponential distribution is the closest approximation to the actual distances that a projectile would travel between collisions if it were in a 2D field of perfectly random, circular scatterers [7]. It is given by:

$$f(r) = \lambda e^{-\lambda r} \tag{2}$$

where the average distance between scattering events is $\frac{1}{\lambda}$.

2.2.3. Energy-Dependent Scattering (EDS)

Various physical models found in refs. [9,19] have scattering rates that depend on differing energy dependencies including $\epsilon^{1/2}$ for elastic acoustic phonon scattering and ionized impurity scattering and $\epsilon^{3/2}$ for warped bands. In this paper, the energy-dependent scattering (EDS) method models a scattering rate that depends on energy. The only random variable is the scattering angle; the time between the scattering events is determined directly from the kinetic energy of the particle. Specifically, the scattering rate γ is proportional to the kinetic energy ϵ to some power n .

$$\gamma \propto \epsilon^n \quad (3)$$

Since the kinetic energy is directly proportional to the squared speed v^2 of the particle, the scattering time t is directly calculated as follows:

$$t = \frac{1}{k(v^{2n})} \quad (4)$$

where k is a constant. To avoid infinite times, a random nonzero initial velocity is chosen at the start of the program. The x and y components of the initial velocity are random numbers between $(-1,1)$. Different values of n are tested. As n approaches zero, the time between scattering events no longer depends on the velocity and becomes constant, so it should reproduce the results of the TDS model.

An exponential dependence of the scattering rate on energy was also tested, where:

$$\gamma \propto e^{\sqrt{\epsilon}} \quad (5)$$

such that:

$$t = Ae^{-kv} \quad (6)$$

where A and k are constants.

2.3. Evaluation of Drift Velocity

The drift velocity is the average motion of particles in the direction of the applied force. For example, in the case of electrons in an isotropic material, the drift velocity is directly proportional to the current, which is the net motion of charge in the direction of the applied electric field. If the direction of the force is in the $-y$ direction, then the numerical derivative of the average y position vs. time will give the net speed of the particles in the direction of the force. For a constant drift velocity, the $\langle y \rangle$ vs. t plot is linear, and the drift velocity is the slope of the linear fit:

$$\langle y \rangle = v_d t + c \quad (7)$$

In Equation (7), the constant c will depend on initial conditions. There are two ways to find the average y position vs. time. The first way is to average the y positions of every run at each step in the simulation. Each step corresponds to a scattering event. Then, the time between scattering events can be averaged for every step over every run. The total time at a given step can be found by accumulating all average times for each step up to that point. This first method works best for the TDS model, when the average time between collisions is relatively constant, meaning that the step number is proportional to simulation time. The second and more exact way to find the average y position vs. time is to sample the data using kinematics. First, the total time of each run is calculated. Next, the total time of the shortest run is chosen as the maximum time (t_{stop}) to sample. Third, a list of sampling times is generated, starting from a given initial time t_{start} and ending at t_{stop} . Next, the y value of every run at each sampling time is calculated by informed interpolation, using kinematics to deduce the position at the exact time desired. This second method is best for

the SDS and EDS models, where the average time between collisions is highly varied and therefore not correlated with the step number.

Other methods for calculating the drift velocity (and other estimators) have been defined by Jacoboni and Reggiani [9]. The method for calculating an estimator for a system that reaches a steady state differs from that used for time-dependent, or transient, phenomena. Nevertheless, some of the steady state methods could still be applied with the additional step of averaging over an ensemble of particles. For example, for a particle that reaches a steady state, its drift velocity can be calculated from one trajectory with an integral of the velocities over the entire simulation time:

$$\vec{v}_d = \frac{1}{T} \sum_{i=1}^N \int_0^{\tau_i} (\vec{v}_{0_i} + \vec{a}t) dt \quad (8)$$

where \vec{v}_d is the drift velocity, T is the total simulation time, N is the number of steps, τ_i is the time of free flight for the given step i , \vec{v}_{0_i} is the initial velocity at that step, and \vec{a} is the acceleration due to the external force.

For a single particle that does not reach a steady state, i.e., constantly increasing in energy, Equation (8) will not settle at a constant value for long periods of time. If, however, several particles are simulated, and the results of the drift velocity calculated in Equation (8) are averaged over the entire ensemble for each step or in time bins, then the result calculated with Equation (7) is reproduced. This method involves more averaging, and the results will be inherently noisier than directly calculating the slope of the position vs. time plot in the direction of the force.

To determine the precision of the results in any ensemble method, we divide the ensemble data into five sub-ensembles, calculate the drift velocity for each, and find the average value and standard deviation [9].

It is also worth noting two methods which will not give an accurate estimation of the drift velocity. The first involves averaging over all y -component velocities of the ensemble of particles just before each scattering event. The final average velocity just before scattering is not equivalent to the drift velocity because the particles are accelerating in the force field. Their net speed in the direction of the applied force will be slower than the final velocity they reach just before scattering. A second method, which builds on the first, would be to calculate the average velocity blue between scattering events:

$$v_d = \frac{\langle v_{y_{final}} \rangle + \langle v_{y_{initial}} \rangle}{2} \quad (9)$$

This result is only true for systems where there is a constant time between scattering events. For systems where there is a distribution of scattering times, including the Drude Model, Equation (9) will over- or underestimate the drift velocity depending on the distribution if one is not careful with the averaging of the initial and final velocities.

We focus on using Equation (7) for calculating the drift velocity of the TDS models which exhibit a constant slope in the $\langle y \rangle$ vs. t plots. For SDS and EDS models, the $\langle y \rangle$ vs. t plots are fit to power laws, and the numerical derivative are also calculated to show the transient behavior of the drift velocity.

3. Results

A constant slope of the $\langle y \rangle$ vs. t plot indicates a constant drift velocity. This was only observed in the time-dependent scattering model. Namely, a constant slope was observed in the time-dependent scattering (TDS) model for the uniform scattering angle (2π range of allowed scattering angles), as well as symmetric and directional exclusion angles. Vertical exclusion angles did not result in a constant drift velocity for the TDS model. The space-dependent scattering (SDS) and energy-dependent scattering (EDS) models do not exhibit a constant drift velocity. Rather, the drift velocity approaches zero in both cases.

3.1. Time-Dependent Scattering (TDS)

Three different distributions of times between scattering events were tested: (1) constant scattering time of 0.5 s, (2) uniform distribution of scattering times between 0 – 1 s, and (3) exponential distribution with relaxation time $\tau = 0.5s$. For comparison, the same average time between collisions, 0.5 s, was chosen for each distribution. The constant time model had the slowest constant drift velocity, averaging at $-2.47 \pm 0.10 \text{ m} \times \text{s}^{-1}$ while the exponential distribution had the fastest constant drift velocity at $-4.93 \pm 0.05 \text{ m} \times \text{s}^{-1}$, as shown in Figure 2. The average drift velocities were calculated by averaging the slopes of 5 trials of 1000 runs each. These results are later compared to the analytical derivation in the Theory section.

In the next sections, the uniform distribution of scattering times will be used to look at the behavior of the drift velocity as the range of scattering angles is limited by different exclusion angles. The first case, the uniform scattering angle, where all scattering angles between $0-2\pi$ are equally probable is shown in Figure 3a.

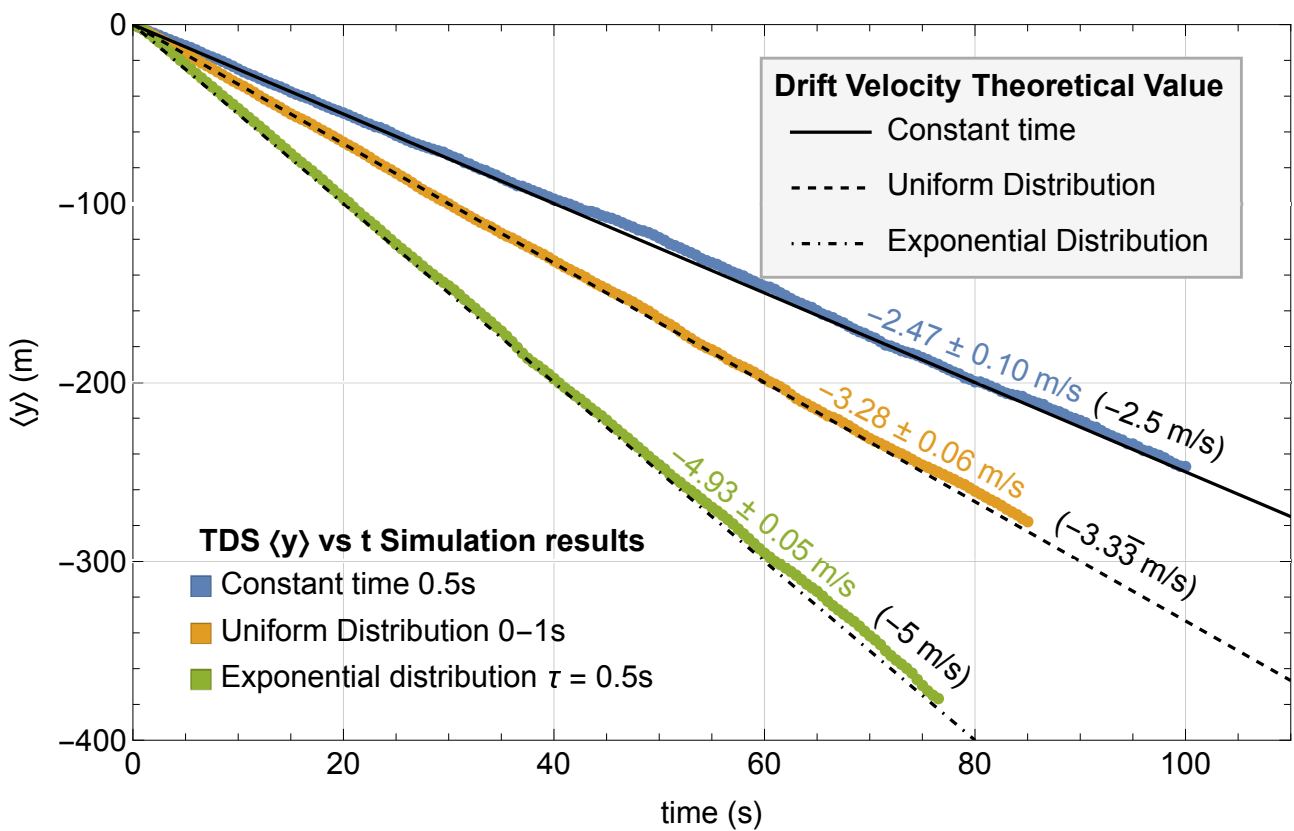


Figure 2. Average y position vs. time for constant, uniform, and exponential time distributions for the time-dependent scattering (TDS) model. The average drift velocities and their standard deviations for each distribution are noted next to the $\langle y \rangle$ vs. t simulation result plot lines with the theoretical values in parentheses. The theoretical results for each are shown by the black lines.

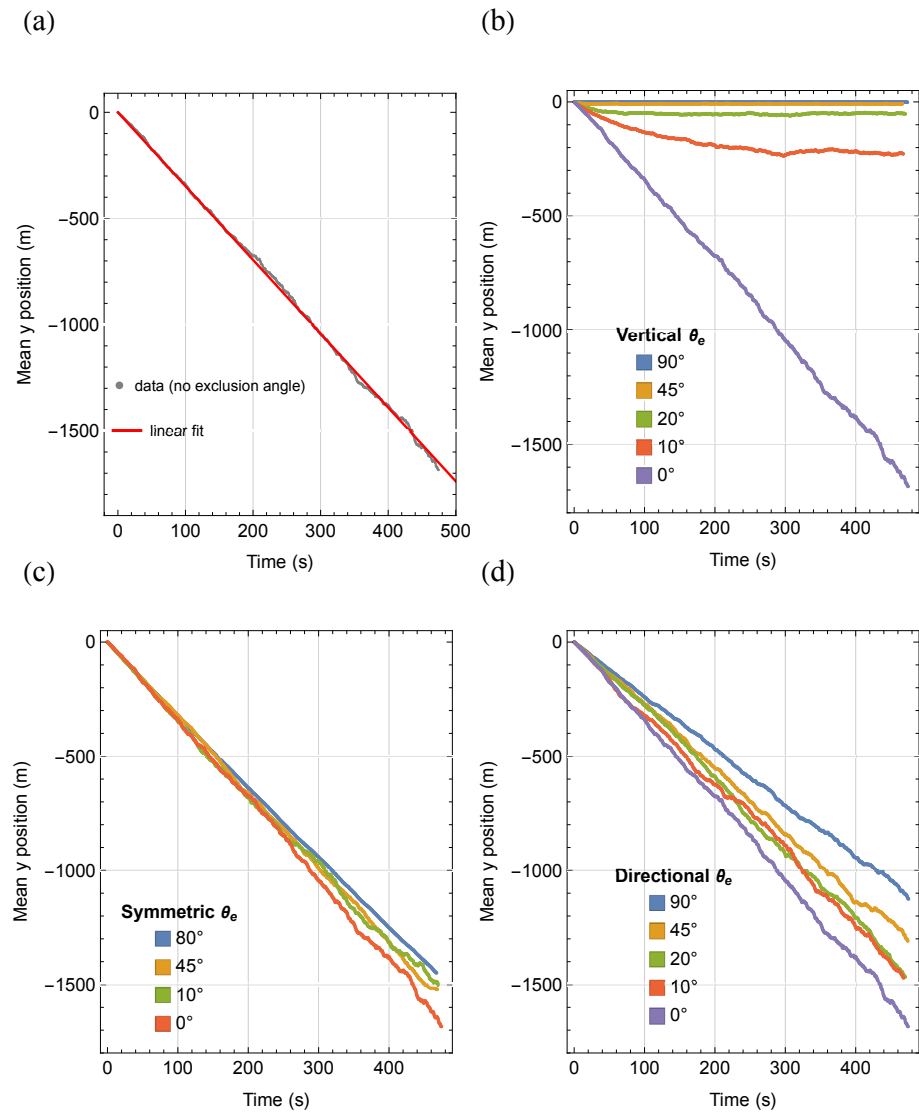


Figure 3. Mean y position vs. time plots for the time scattering model, where $\vec{a} = -10 \text{ m} \times \text{s}^{-2} \hat{y}$. (a) The uniform, 2π range of allowed scattering angles, has a constant drift velocity of about $-3.3 \text{ m} \times \text{s}^{-1}$. (b) Vertical exclusion angles, which disallow scattering in the $-\hat{y}$ direction, for $\theta_e = 0, 10, 20, 45,$ and 90 degrees. The particles reach a constant mean y position for $\theta_e > 0$. The 0° line refers to no exclusion angle, which is the same as the uniform 2π distribution. (c) Symmetric exclusion angle model, where the particle is restricted from scattering in the $\pm y$ directions for $\theta_e = 0, 10, 45$ and 80 degrees. A constant drift velocity returns, and remains about the same as the uniform model for all θ_e . (d) Directional exclusion angles, where scattering is disallowed in the direction of the particles' motion when scattering for $\theta_e = 0, 5, 20, 45$ and 90 degrees. The drift velocity decreases as θ_e increases.

3.1.1. Vertical Exclusion Angle

Vertical exclusion angles of $5, 10, 20, 30, 40, 50, 60, 70, 80,$ and 90° were tested. For every vertical exclusion angle, the slope of the $\langle y \rangle$ vs. t began to decrease and approach zero. Therefore, no constant drift velocity was obtained with the vertical exclusion angle model. The rate at which the velocity approaches zero depends on the vertical exclusion angle. The smaller the exclusion angle, the slower the $\langle y \rangle$ vs. t plot approached a slope of zero. The simulation was run for a longer time for smaller angles. At a long enough time, the $\langle y \rangle$ vs. t plot would reach a horizontal asymptote at a fixed y position. This is the maximum average displacement of the particles in space. For the 5° exclusion angle, the maximum average distance was about $y = -1000 \text{ m}$. For 10° it was about $y = -230 \text{ m}$. See Figure 3b.

3.1.2. Symmetric Exclusion Angle

The symmetric exclusion angle model, which also prohibited up-scattering as well as down-scattering for the same range of angles, resulted in a constant drift velocity. Symmetric exclusion angles of 10, 45, and 80° were tested. The slope of the $\langle y \rangle$ vs. t plot remained about the same for each exclusion angle: about $3.3 \pm 0.9 \text{ m} \times \text{s}^{-1}$. The slopes of the mean y position vs. time plots for the symmetric exclusion angle model were closest to the velocity of the model with no exclusion angle. There does not seem to be a correlation between symmetric exclusion angle and drift velocity. However, the standard deviation of the velocity for greater exclusion angles does decrease. This is due to the fact that there is a smaller range of angles and therefore less variation in the y component of the velocity after scattering. See Figure 3c.

3.1.3. Directional Exclusion Angle

In the directional exclusion angle program, the constant drift velocity returned, with different values for different ranges of angles. Directional exclusion angles of 5, 10, 20, 45, and 90° were tested. As the range of allowed angles decreased, meaning as the directional exclusion angle increased, the drift velocity decreased. See Figure 3d.

To calculate the drift velocities, five trials were completed for each exclusion angle in every model that exhibited a constant $\langle y \rangle$ vs. t slope, for 500 runs and 1000 steps each. The average y position vs. time was found by averaging the y position of every run at each step. The time at each step was also calculated by averaging the total time of every run at each step.

Figure 3 shows the average y position vs. time for selected exclusion angles in each model: vertical, symmetric, and directional exclusion angles. Figure 4 shows the calculated steady-state, constant drift velocities, and their standard deviations for each model and exclusion angle. The drift velocity of the vertical exclusion angles is plotted as zero.

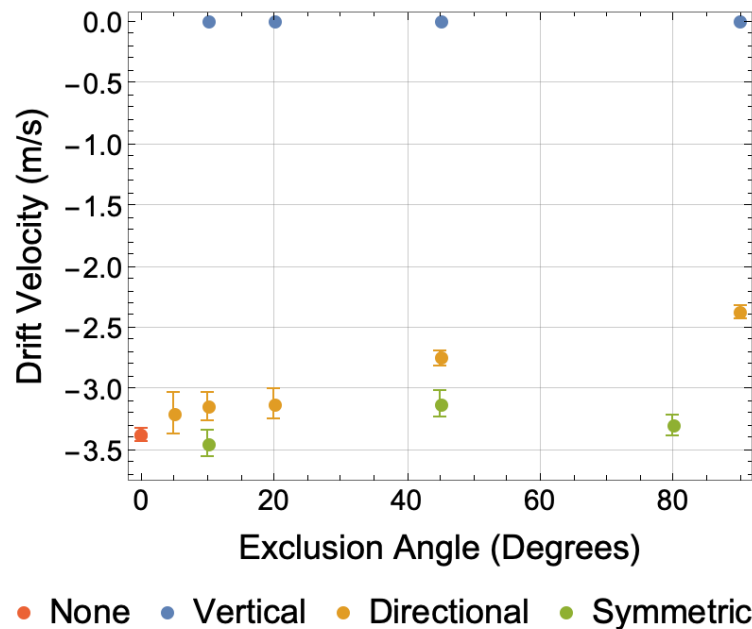


Figure 4. Exclusion angle (θ_e) vs. drift velocity (v_d) for all time scattering models. The value for “None” exclusion angle (red) is $-3.3 \text{ m} \times \text{s}^{-1}$. The v_d for vertical exclusion angles (blue) is zero. The directional exclusion angle (orange) v_d slows as θ_e increases. The symmetric exclusion angle (green) v_d remains about the same for all θ_e .

3.2. Space-Dependent Scattering (SDS)

Three different distributions were used to determine the distance between scattering events in the SDS model: constant distance (1.0 m), nearest neighbor (Equation (1)),

$\rho = 0.25$), and exponential (Equation (2), $\lambda = 1$). For comparison, distributions with the same average distance of 1.0 m were chosen. The $\langle y \rangle$ vs. t plots for each distribution were fit to a power law function:

$$\langle y \rangle = at^b + c \tag{10}$$

where a and b are fitting constants, and c , which corresponds to the initial position, was set to the actual initial condition of the system $y_0 = 0$ m. Figure 5 shows the average position $\langle y \rangle$ vs. t for each distribution and the corresponding fits.

A power law average position plot means that the drift velocity of the system of particles decreases with time, approaching zero asymptotically. This is shown by a simple derivative of Equation (10).

$$v_d = abt^{b-1} \tag{11}$$

The drift velocity vs. time was calculated by taking the derivative of the power law fit $\langle y \rangle$ vs. t functions. These were plotted and compared with numerical derivatives of the data (see Figure 5). Taking the limit as $t \rightarrow \infty$, the drift velocity approaches zero for all distributions, given that b is less than 1.0. This result was predicted previously by Wolfson et al. in their rain stick model [20], which is the periodic lattice version of the random SDS model in this present study. The results presented here go further to exhibit the time behavior of the transient drift velocity. The exponent b for all power law fits of the vertical position vs. time plot is between 0.61–0.66, which is about 2/3. This corresponds to a drift velocity that decays with time to the power $-1/3$.

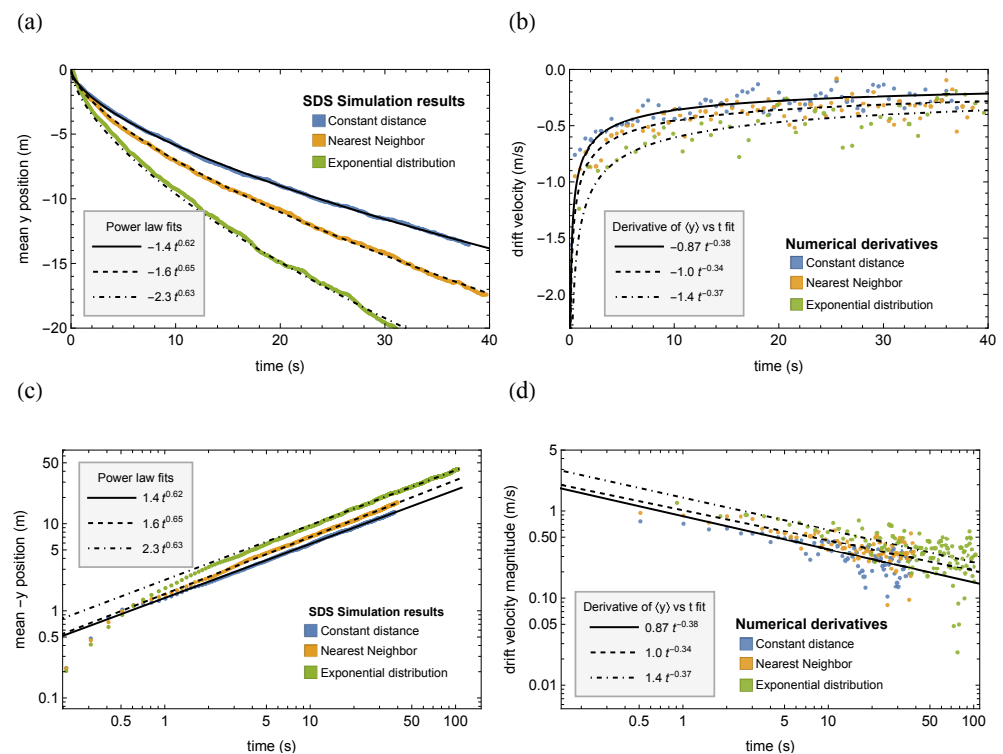


Figure 5. (a) The average y position vs. time (t) for the SDS models—constant distance, nearest neighbor distribution, and exponential distribution—plotted with power law fits, shown in the legend. The average distance for each model is the same: 1 m. Each data point is the average over 1000 runs. The constant distance and nearest neighbor distribution were run for 1000 scattering events. The exponential distribution was run for 5000 scattering events. (b) v_d vs. time shown with numerical derivatives of the $\langle y \rangle$ vs. t data and analytic derivatives of the power law fits. (c) A log–log scale plot of the average $-y$ vs. time data with fits. (d) A log–log scale plot of the $|v_d|$ vs. time data with fits. Both show the non-power law behavior at the beginning of the simulation as the particles go from initial condition to steady state.

To further investigate the power law fits of the vertical position vs. time plots, different densities of the NND were tested.

Nearest Neighbor Distribution

Six different densities ρ were tested: 0.25, 0.5, 1, 10, 100, and 1000 scatterers per m^2 . For each density, five trials with a minimum of 500 runs of 500 steps each were performed. Figure 6 shows the fitting parameters a and b for the power law fits of the $\langle y \rangle$ vs. t plots for each density. For higher densities, the a parameter drops significantly, while the b parameter, the power, remains relatively the same: about 0.67. The a parameter was fit to an inverse power law function. Since the a parameter decreases with ρ , the rate of decrease in the drift velocity vs. time is slower for higher densities.

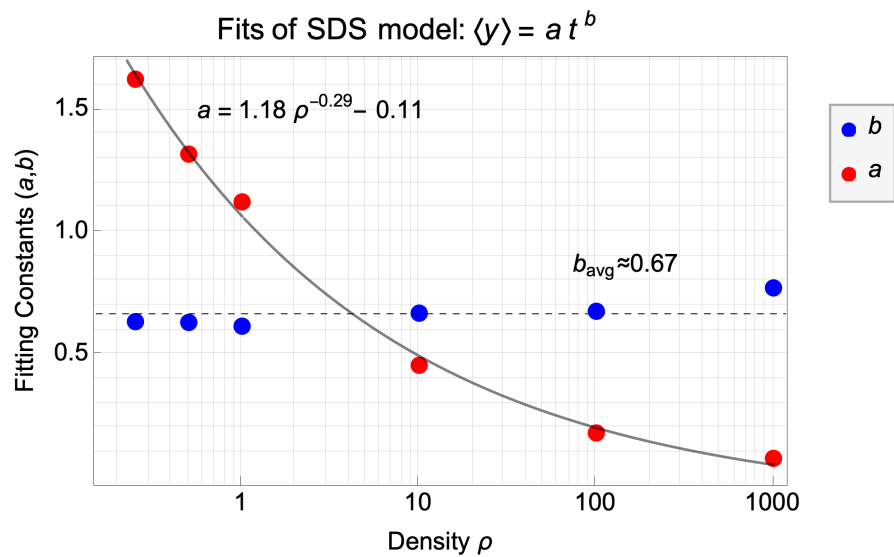


Figure 6. Fitting constants (a, b) vs. density ρ for SDS using the nearest neighbor distribution of distances between scattering. The a constants were fit to an inverse power law function to show the general decreasing trend as ρ increases. The b powers remain about the same for all ρ . The density axis is log-scaled.

3.3. Energy-Dependent Scattering (EDS)

Exponential ($A = 0.1$ in Equation (6)), linear ($k = 10, n = 1$), and power law ($k = 10, n = 0.5$) energy-dependent models are examined, referring to Equation (4). The $\langle y \rangle$ vs. t plots were fit to the power law function (Equation (10)). See Figure 7a. Taking the numerical derivative of the average y position plot and the analytic derivative of the fit, it is evident that the drift velocity will also approach 0 for all models at long times (Figure 7b).

The power law scattering frequency dependence, where $t = \frac{1}{kv^{2n}}$, can be taken to the limit of $n \rightarrow 0$. When $n = 0$ the scattering rate is no longer dependent on the velocity of the particle, and we reproduce the constant time scattering model. The $\langle y \rangle$ vs. t plot for the power law dependence model can also be fit to a power law function: $\langle y \rangle = at^b + c$. The constant c should be about zero for every fit, since the initial y position is zero for each model. The exponent b and scaling constant a were plotted as a function of n .

We expect b to approach 1 as $n \rightarrow 0$ because the constant time scattering model has a linear $\langle y \rangle$ vs. t plot (constant drift velocity).

The fitting exponent b is about the same for different values of k , however, the scaling constant a is greater for lower values of k . See Figure 8.

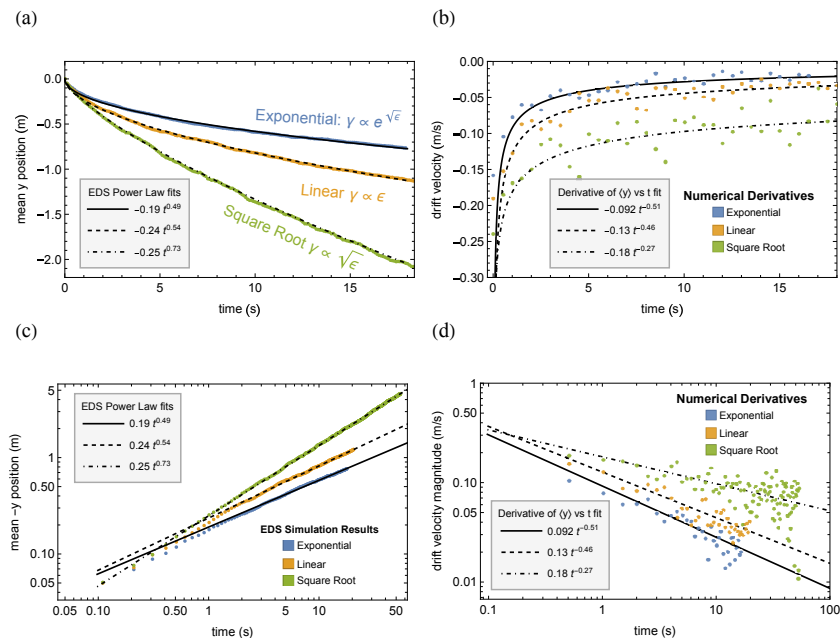


Figure 7. (a) Mean y position vs. time for different EDS models: exponential (blue), linear (orange), and square root (green), with power law fits $\langle y \rangle = at^b + c$. (b) Drift velocity v_d vs. time plotted with the numerical derivative of the $\langle y \rangle$ vs. t position data (points) and the analytic derivative of the position power law fits (lines). Both show that the drift velocity asymptotically approaches zero for all EDS models. (c) A log–log scale plot of the average $-y$ vs. time data with fits. (d) A log–log scale plot of the $|v_d|$ vs. time data with fits.

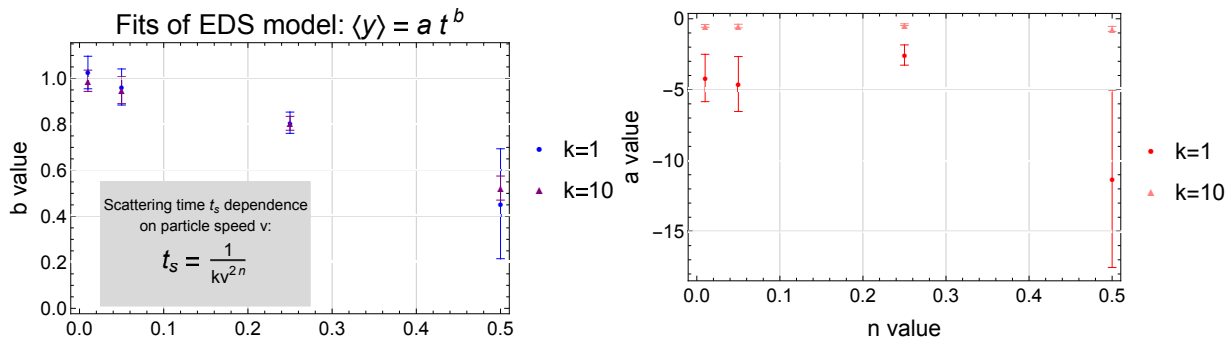


Figure 8. Fitting parameters for the $\langle y \rangle$ vs. t plot of the power law energy-dependent model, plotted for different values of n . $\langle y \rangle = at^b + c$.

4. Theory and Discussion

In this section, we introduce the method of analytically calculating the drift velocity by averaging over the motion of the particles. First, we compare the results of this method to the Drude model. Second, we generalize the result for any distribution of times between scattering events for the TDS method. Third, we analyze the results of the vertical, symmetric, and directional exclusion angle models. Fourth, we examine the SDS and EDS models, where the drift velocity goes to zero.

4.1. Drude Model Drift Velocity

In the Drude model, the only forces on the electrons are supplied by a uniform force field and random scatterers. The balance of these two forces will be what produces a constant drift velocity. The drift velocity for the Drude model, which assumes a constant relaxation time τ between scattering events, has been well defined and calculated [4,5].

The result is that the change in momentum per electron equals the external force minus an effective force due to scattering.

$$\frac{d\vec{p}(t)}{dt} = \vec{F}(t) - \frac{\vec{p}(t)}{\tau} \tag{12}$$

Here, $\vec{p}(t)$ is the momentum and $\vec{F}(t)$ is the external force per electron. The last term in Equation (12) is the effective force per electron due to scattering. It acts as a frictional damping term in the equation of motion. A constant drift velocity arises when $\frac{d\vec{p}(t)}{dt} = 0$. Plugging in $\vec{F}(t) = m\vec{a}$ and $\vec{p}(t) = m\vec{v}$ and rearranging, we arrive at:

$$\vec{v}_{d_{Drude}} = \vec{a}\tau \tag{13}$$

Unlike the Drude Model, the models presented in this paper all assume elastic scattering, meaning that the particles do not lose energy during a collision. However, some elastic scattering models do arrive at a constant drift velocity. This can be seen most clearly in the TDS model.

There are three factors in both the Drude and TDS models that produce a constant drift velocity:

1. A constant, uniform external force;
2. An unchanging average time between scattering events;
3. A momentum reset on average after scattering.

Every model presented in this research satisfies the first condition. The SDS and EDS models do not satisfy the second condition and have a drift velocity which changes (and even slows) with time. In the TDS model, the third condition is affected when the range of scattering angles is limited with exclusion angles.

4.2. TDS Models

The TDS models are all characterized by an average constant time between collisions. Different ranges of scattering angles are also considered, as shown in Figure 1. The TDS model with a uniform scattering angle satisfies the three conditions above and results in a constant drift velocity. By changing the range of exclusion angles, the average momentum of the particles after scattering will no longer be zero in some cases. This changes the drift velocity behavior.

4.2.1. Uniform Scattering Angle

In the uniform scattering angle TDS model (see Figure 1a), when the particle can scatter in any direction with equal probability, the average momentum is still reset after every collision, as in the Drude Model. If there is an average time between scattering and a constant and uniform external force in the $-y$ direction, then the average velocity between scattering events in the direction of the force, $\langle v_y \rangle_{flight}$, will be constant for all time. This velocity represents the average motion of the particles in the direction of the force, which is precisely the drift velocity.

$$v_{d_{TDS}} = \langle v_y \rangle_{flight} \tag{14}$$

The average y velocity between scattering events, i.e., during free flight, $\langle v_y \rangle_{flight}$ is the average y displacement of the particle divided by the average time of free flight (between scattering events):

$$\langle v_y \rangle_{flight} = \frac{\langle y \rangle_{flight}}{\langle t \rangle_{flight}} \tag{15}$$

In general, the average value of a kinematic variable f with a probability density function of scattering times $D(t)$ is:

$$\langle f(t) \rangle = \int f(t)D(t)dt \tag{16}$$

where the distribution is assumed to be normalized and the integral is over the range of the distribution. The drift velocities for each distribution of scattering times, exponential, constant and uniform, each with an average time of 0.5 s between collisions, are calculated below.

Exponential distribution of scattering times. For the TDS model with an exponentially distributed scattering time ($D_{TDS-E}(t) = \frac{1}{\tau}e^{-t/\tau}$), the drift velocity can then be calculated as follows:

$$\langle y \rangle_{flight} = \int_0^\infty y(t)D(t) dt = \int_0^\infty \frac{1}{2\tau}at^2e^{-t/\tau} dt = a\tau^2 \tag{17}$$

$$\langle t \rangle_{flight} = \int_0^\infty tD(t) dt = \int_0^\infty \frac{t}{\tau}e^{-t/\tau} dt = \tau \tag{18}$$

Therefore, from Equations (14) and (15), the drift velocity is:

$$v_{d_{TDS-E}} = a\tau \tag{19}$$

This result is consistent with the drift velocity found with the TDS Monte Carlo model with an exponential distribution of scattering times and relaxation time τ . With an acceleration = $10 \text{ m} \times \text{s}^{-2}$ and a relaxation time of $\tau = 0.5 \text{ s}$, then the system arrives at a constant drift velocity of $a\tau = 5 \text{ m} \times \text{s}^{-1}$. The calculated value in Figure 2 and Section 4.2.1, $-4.93 \pm 0.05 \text{ m} \times \text{s}^{-1}$, which is slightly less than the analytical value. The difference could be due to the initial conditions of the simulated model, which would bias the linear fit to have a smaller slope.

It is worth noting that this analytical result for the TDS-exponential distribution model is the same as the Drude Model drift velocity in Equation (13). This is to be expected because the distribution of scattering times for the Drude model is exponential with a relaxation time τ , as shown in Ashcroft’s problem 1 [4].

Constant time scattering. Referring to Equation (16), the distribution for the constant time scattering model is

$$D_{TDS-C}(t) = \delta(t - t^*) \tag{20}$$

where t^* is the constant time between scattering events. This yields, $\langle y \rangle_{flight} = \int_0^\infty \frac{1}{2}at^2\delta(t - t^*) dt = \frac{1}{2}a(t^*)^2$ and $\langle t \rangle_{flight} = t^*$. The drift velocity from Equation (15) is:

$$v_{d_{TDS-C}} = \langle v_y \rangle_{flight} = \frac{1}{2}at^* \tag{21}$$

This is consistent with the result from simulation. Specifically, when the time between events is 0.5 s, and the acceleration due to the force is $10 \text{ m} \times \text{s}^{-2}$, the drift velocity is measured to be about $2.47 \pm 0.07 \text{ m} \times \text{s}^{-1}$, which is within error of the analytical result of $\frac{1}{2}at^* = 2.5 \text{ m} \times \text{s}^{-1}$.

Uniform distribution of scattering times. For the uniform distribution of scattering times, the probability density function is:

$$D_{TDS-U}(t) = \frac{1}{t_{max} - t_{min}} \tag{22}$$

for the range $t_{min} < t < t_{max}$. From Equation (16), where $y(t) = \frac{1}{2}at^2$ this gives $\langle y \rangle = \frac{1}{6}a(t_{max} - t_{min})^2$ and $\langle t \rangle = \frac{1}{2}(t_{max} + t_{min})$. Then, using Equation (15):

$$v_{d_{TDS-U}} = \langle v_y \rangle_{flight} = \frac{1}{3}a(t_{max} - t_{min}) \tag{23}$$

For $a = 10 \text{ m} \times \text{s}^{-2}$, $t_{min} = 0\text{s}$, and $t_{max} = 1\text{s}$, the value of the drift velocity should be $3.3 \text{ m} \times \text{s}^{-1}$. This is consistent with the drift velocity calculated using the Monte Carlo simulation: $3.3 \pm 0.1 \text{ m} \times \text{s}^{-1}$.

Even though the average time between collisions is the same for the uniform distribution and constant scattering time models, 0.5 s in each case, the drift velocity for the latter is smaller. The difference is that in the uniform distribution model, there is a possibility for scattering times that are longer than 0.5 s. Since the particle is accelerating, these longer times will have more weight, contributing more to the net speed than the shorter times will subtract from it.

With a uniform scattering angle, the average momentum is reset after scattering. Therefore the TDS models are able to achieve a constant drift velocity even with elastic scattering. A constant drift velocity would also occur with elastic scattering if the the momentum lost in the y direction is completely redirected into the x direction. The redirection of the momentum from the y to the x direction replaces the loss of kinetic energy of the particle implied with inelastic scattering models. This is seen in the symmetric exclusion angle model below.

4.2.2. Vertical Exclusion Angle

Once a vertical exclusion angle is introduced, as shown in Figure 1b, the average momentum after scattering is no longer reset. Because the particle is excluded from scattering in the direction of the force, the average momentum after collisions is in the opposite direction of the force. The average momentum after scattering $\langle p \rangle_{scat}$ can be calculated by averaging over all allowed scattering angles.

$$\langle \vec{p} \rangle_{scat} = \frac{\int (p_x(\theta) \hat{x} + p_y(\theta) \hat{y}) d\theta}{\int d\theta} \tag{24}$$

The integral of the average momentum is evaluated over the range of allowed scattering angles: $-\frac{\pi}{2} + \theta_e$ to $\frac{3\pi}{2} - \theta_e$, where θ_e is the exclusion angle. The normalization integral in the denominator is therefore $2(\pi - \theta_e)$. Plugging in $mv \cos \theta$ for p_x and $mv \sin \theta$ for p_y , we get an average momentum of:

$$\langle \vec{p} \rangle_{scat} = \frac{mv \sin \theta_e}{\pi - \theta_e} \hat{y} \tag{25}$$

This momentum depends on the incoming speed v of the particle.

In this model, the drift velocity slows down, and the average position of the particles even gets “stuck” at a given y value. The average velocity after scattering $\langle \vec{v} \rangle_{scat}$ is the average momentum divided by mass:

$$\langle \vec{v} \rangle_{scat} = \frac{v \sin \theta_e}{\pi - \theta_e} \hat{y} \tag{26}$$

It is important to note that $\langle \vec{v} \rangle_{scat}$ depends on the incoming speed of the particle v . In a model with elastic collisions, the speed of the particle is constantly increasing. After each scattering event, $\langle \vec{v} \rangle_{scat}$ will approach the average velocity gained during free flight $\langle \vec{v} \rangle_{flight}$.

When $\langle \vec{v} \rangle_{scat} = \langle \vec{v} \rangle_{flight}$, then the system’s average displacement will stop changing and settle at a maximum value. With no net motion of the particles, the drift velocity of the TDS model with any vertical exclusion angle $> 0^\circ$, $v_{d_{TDS-v}}$, will approach zero.

$$v_{d_{TDS-v}} \rightarrow 0. \tag{27}$$

4.2.3. Symmetric Exclusion Angles

The symmetric exclusion angle is shown in Figure 1c. In this case, the particle is excluded from scattering in the $\pm y$ directions for a given range of angles given by the half angle θ_e . The average momentum after scattering can be calculated by averaging over all of the allowed scattering angles. The ranges of allowed scattering angles are equally probable and in opposite directions, so the average momentum after scattering is zero. This

means that the momentum is again reset on average after the scattering event, as it was for a uniform distribution of scattering angles between $0-2\pi$. Therefore, the analytic drift velocity will be the same as for the uniform scattering angle models, and will simply depend on the distribution of times between scattering events. The drift velocity is calculated by finding the average y velocity between collisions as before.

There is one distinctive property of the symmetric exclusion angle model: the variance in the simulated drift velocity decreases as θ_e increases. This can be seen if we take θ_e to the extreme limit where the particle is only scattered in a direction perpendicular to the external force. In this case, all of the momentum in the y direction is transferred to the x direction after every scattering event and there is no variance in the drift velocity of the particles.

An even more extreme case is that where the particle is only allowed to scatter in the $+x$ direction, which is perpendicular to the force. The net momentum after scattering is no longer zero; it is in the positive x direction. However, a constant drift velocity, which is measured in the direction of the force, could also be achieved in this case. Therefore, it is only necessary that the momentum in the y direction is reset after scattering in order for the system to reach a constant drift velocity.

4.2.4. Directional Exclusion Angles

When the exclusion angle depends on the direction of motion of the particle, as in the case of the directional exclusion angle model (Figure 1d), then the constant drift velocity returns. In fact the drift velocity can be tuned by adjusting the range of excluded angles. The greater the θ_e , the smaller the drift velocity, as seen in the slopes of the $\langle y \rangle$ vs. t plot in Figure 3d. The drift velocities plotted in Figure 4 shows an almost linear correlation between θ_e and v_d . In fact, when the directional exclusion angles are repeated for a constant time TDS model, the linear regression is a very close fit.

Several attempts have been made to analytically derive the relationship between θ_e and v_d for directional exclusion angles. One way involves conditional probability, where the distribution of allowed angles on average after scattering is evaluated recursively. The scattering angle probabilities are step functions centered around the direction of flight at scattering. Deriving the average distribution of scattering angles after N scattering events (steps) involves adding N uniform distributions centered at different angles. According to the central limit theorem, the distribution of scattering angles on average should approach a normal distribution. A quick visualization of the average range of scattering angles after N steps shows that it quickly randomizes after a few steps, and all scattering angles from $0 - 2\pi$ become equally probable. The angles randomize quicker for smaller θ_e . This would explain why the model reaches a constant drift velocity for all directional exclusion angles; if after a certain number of steps all scattering angles are equally probable on average, then the momentum effectively resets after collisions. The average time between scattering events being constant would mean that the models would all gain the same velocity on average after each scattering event. Nevertheless, the analytic solution for the relationship between directional θ_e and v_d still remains an open question.

4.3. SDS and EDS Models

A uniform distribution of scattering angles between $0-2\pi$ was used for both SDS and EDS models, so the average momentum after scattering is also zero. However, in both models, the drift velocity approaches zero for long periods of time. This result is explained for the space scattering model by ref. [20]: if the system is purely elastic and the particles do not lose energy between collisions, then the material will become “optically thick” as particles reach fast speeds, and the drift velocity will approach zero. As particles gain kinetic energy, the time between collisions approaches zero, so they have negligible time to respond to the applied force. For the SDS model where a constant distance or random distance between scattering events is chosen, higher speeds naturally result in shorter intervals between scattering events. In the EDS model, the scattering rate is set up

to increase as the speed of the particle increases. With elastic collisions, the kinetic energy of the particles is constantly increasing, resulting in faster scattering rates and smaller free-flight times that approach zero.

For the SDS, the velocity gained during free flight can be analytically calculated and shown to depend on the speed of the particle. For a constant distance l between scattering events, the time between collisions is $t = l/v$, where v is the speed of the particle right before scattering. The kinematic variable $y = \frac{1}{2}at^2 = \frac{al^2}{2v^2}$, which is also $\langle y \rangle_{flight}$ for a constant distance l . The average time between collisions is also $\langle t \rangle_{flight} = l/v$ from Equation (15):

$$v_{d_{SDS}} = \langle v_y \rangle_{flight} = \frac{1}{2} \frac{al}{v} \tag{28}$$

As the speed increases to $v \gg al$, the drift velocity for the SDS model, $v_{d_{SDS}}$ will approach zero:

$$v_{d_{SDS}} \rightarrow 0 \tag{29}$$

The EDS model has set relations between the time between scattering and the velocity. For the power law relation, Equation (3), recalling that $\gamma \propto 1/t$ and $\epsilon \propto v^2$, the time between scattering events is $t \propto 1/v^{2n}$. The velocity gained on average during free flight for the EDS power law model is:

$$v_{d_{EDS-pl}} = \langle v_y \rangle_{flight} \propto \frac{1}{2} \frac{a}{v^{2n}} \tag{30}$$

The drift velocity again depends on the speed of the particle. For higher values of the exponent n , the drift velocity will approach 0 at a faster rate. In the limit that $n = 0$, we reproduce the TDS model with a constant scattering rate.

A similar analysis can be made for the exponential dependence of the scattering rate on energy, given by Equation (5). Here, $t \propto e^{-v}$

$$v_{d_{EDS-exp}} = \langle v_y \rangle_{flight} \propto \frac{1}{2} ae^{-v} \tag{31}$$

The drift velocity will again approach zero as v increases.

$$v_{d_{EDS}} \rightarrow 0 \tag{32}$$

5. Conclusions

This research has shown that it is possible to achieve a constant drift velocity with elastic scattering. The time-dependent scattering model, where the average time between collisions was constant, immediately resulted in a constant drift velocity. Changing the range of scattering angles alters the drift velocity results. By excluding a range of scattering angles in the direction of the applied force, the particles reached a maximum average displacement and their average velocity reached zero in that direction. When the same range of scattering angles was excluded in opposite directions, in the direction of the force and against it, then the constant drift velocity returned with approximately the original value it had with a uniform 2π distribution of allowed scattering angles. Finally, a directional exclusion angle allows for the drift velocity to be tuned, decreasing as the exclusion angle in the direction of the particle’s motion increases. The directional exclusion angle model is most like the range of angles that classical scattering would allow, where the direction of propagation after scattering depends on its impact parameter. The analytical derivation of the relationship between the directional exclusion angle and the drift velocity remains an open question.

The space-dependent scattering and energy-dependent scattering models do not arrive at a constant drift velocity. These two models are related in that, as the kinetic energy of the particle increases, the time between collisions decreases. This means that the force on the particle has a negligible effect on the change in speed of the particle between flights.

The $\frac{1}{2}at^2$ term becomes much smaller than vt at short times and high speeds. This causes the average velocity of the particles in the direction of the force to decrease with time.

Three-dimensional models and models with elastic boundaries were also considered in this study. The drift velocity of the particles in these models is the same as in the two-dimensional and boundary-less models with similar parameters. This means that the diffusion of energy in a third dimension does not change the drift velocity in the direction of the force. Elastic boundaries, where the particle simply reflects its velocity, only confines the horizontal position of the particles and has no effect on their overall average vertical motion in the direction of the force.

6. Future Research

In addition to deriving the relationship between drift velocity and directional exclusion angle, this study opens up several other questions for further research. The scatterers in this study were chosen randomly. How would the drift velocity behavior change for a perfectly periodic lattice of scatterers? The range of ordering from a completely periodic to a completely random set of scatterers could be investigated. It could still be possible to arrive at a drift velocity with the SDS model by introducing a scatterer density gradient that decreases in the direction of the force. In this paper, we have only presented a few simple models that lead to a variety of drift behaviors. However, it opens a door to the possibility that there are many more models that could lead to rich behavior with elastic scattering. Some of these could be more realistic physical scattering models such as those that include angle-dependent scattering rates as well as models based on hard and soft sphere kinetics. Finally, to bring the results of this study to the experimental realm, one could use these elastic scattering models to predict or classify the change in transient drift velocity behavior of materials as elastic scatterers are added, for example, by doping with ionized impurities.

Author Contributions: Conceptualization, N.A.M.; Methodology, R.M.M. and N.A.M.; Formal analysis, R.M.M.; Investigation, R.M.M. and N.A.M.; Writing—original draft, R.M.M.; Writing—review & editing, N.A.M.; Visualization, R.M.M.; Supervision, N.A.M.; Project administration, N.A.M. All authors have read and agreed to the published version of the manuscript.

Funding: The research was funded by VSL and ONR, Grant N00014-20-1-2317.

Data Availability Statement: No new data were created or analyzed in this study. Data sharing is not applicable to this article.

Acknowledgments: The authors would like to thank Ian L. Pegg, Lorenzo Resca, Helen McDonough, Luis Aguinaga, Ashraful Haque, Virginia Jarvis, and Ian Chi for their advice and contributions to this research.

Conflicts of Interest: The authors declare no conflict of interest.

Abbreviations and Symbols

The following abbreviations and symbols are used in this manuscript:

TDS	Time-Dependent Scattering
SDS	Space-Dependent Scattering
EDS	Energy-Dependent Scattering
TDS-E	Exponential distribution of scattering times for TDS model
TDS-C	Constant scattering time for TDS model
TDS-U	Uniform distribution of scattering times for TDS model
TDS-V	Vertical Exclusion angle for TDS model
EDS-pl	Energy-Dependent Scattering power law model
EDS-exp	Energy-Dependent Scattering exponential model
NND	Nearest Neighbor Distribution

A	Parameter in the EDS model (coefficient)
a	Acceleration magnitude, Fitting constant (coefficient)
\vec{a}	Acceleration vector
b	Fitting constant (power)
c	Fitting constant (initial condition)
ϵ	Kinetic energy
\vec{F}	Force vector
γ	Scattering rate
k	Parameter in the EDS model
l	Constant distance in the SDS model
λ	Parameter in the exponential distribution
m	Mass of particle
N	Total number of steps
n	Parameter in the EDS model (power)
\vec{p}	Momentum
p_x	x -component of the momentum
p_y	y -component of the momentum
$\langle \vec{p} \rangle_{scat}$	Average momentum after scattering
r	Radial distance
ρ	Number density of scatterers
T	Total simulation time
t	Scattering time, Simulation time
t^*	Constant time between scattering events for TDS model
t_{max}	Maximum time in Uniform Distribution for TDS model
t_{min}	Minimum time in Uniform Distribution for TDS model
t_{start}	Initial time for sampling method
t_{stop}	End time for sampling method
$\langle t \rangle_{flight}$	Average time of free flight (between scattering events)
τ	Relaxation time
τ_i	Time of free flight given step i
θ	Scattering angle after collision
θ_e	Exclusion angle
v	Speed
\vec{v}	Velocity
v_d	Drift velocity
v_x	x -component of the velocity
v_y	y -component of the velocity
\vec{v}_{0_i}	Initial velocity at step i
$\langle \vec{v} \rangle_{flight}$	Average velocity gained during free flight
$\langle \vec{v} \rangle_{scat}$	Average velocity after scattering
x	Horizontal position
y	Vertical position
$\langle y \rangle$	Average y position
$\langle y \rangle_{flight}$	Average displacement in y direction during free flight

References

- Zou, Y.; Esmailpour, H.; Suchet, D.; Guillemoles, J.F.; Goodnick, S.M. The role of nonequilibrium LO phonons, Pauli exclusion, and intervalley pathways on the relaxation of hot carriers in InGaAs/InGaAsP multi-quantum-wells. *Sci. Rep.* **2023**, *13*, 5601. [[CrossRef](#)] [[PubMed](#)]
- Jin, W. High Electric Field Transport Characteristics in Field-Effect Transistors Based on Monolayer/Few-Layer MoS₂. *IEEE Trans. Electron. Devices* **2023**, *70*, 3992–4000. [[CrossRef](#)]
- Yeoh, K.H.; Ong, D.S. Steady-state and transient electron transport in silicon: From bulk to monolayer. *AIP Conf. Proc.* **2017**, *1877*, 080003. [[CrossRef](#)]
- Ashcroft, N.W.; Mermin, N.D. *Solid State Physics*; Saunders College: Philadelphia, PA, USA, 1976.
- Simon, S.H. *The Oxford Solid State Basics*; OUP Oxford: Oxford, UK, 2013.
- Kittel, C.; McEuen, P. *Introduction to Solid State Physics*; John Wiley & Sons: Hoboken, NJ, USA, 2018.
- Lipperheide, R.; Weis, T.; Wille, U. Generalized Drude Model: Unification of Ballistic and Diffusive Electron Transport. *J. Phys. Condens. Matter* **2001**, *13*, 3347. [[CrossRef](#)]

8. Srivastava, A.; Srivastava, P.; Srivastava, A.; Saxena, P. Atomistic nonlinear carrier dynamics in Ge. *Sci. Rep.* **2023**, *13*, 5630. [[CrossRef](#)] [[PubMed](#)]
9. Jacoboni, C.; Reggiani, L. The Monte Carlo Method for the Solution of Charge Transport in Semiconductors with Applications to Covalent Materials. *Rev. Mod. Phys.* **1983**, *55*, 645. [[CrossRef](#)]
10. Ganose, A.; Park, J.; Faghaninia, A.; Woods-Robinson, R.; Persson, K.; Jain, A. Efficient Calculation of Carrier Scattering Rates from First Principles. *Nat. Commun.* **2021**, *12*, 2222. [[CrossRef](#)] [[PubMed](#)]
11. Bird, G.A. Monte Carlo simulation of gas flows. *Annu. Rev. Fluid Mech.* **1978**, *10*, 11–31. [[CrossRef](#)]
12. Borgnakke, C.; Larsen, P.S. Statistical collision model for Monte Carlo simulation of polyatomic gas mixture. *J. Comput. Phys.* **1975**, *18*, 405–420. [[CrossRef](#)]
13. Koura, K. A set of model cross sections for the Monte Carlo simulation of rarefied real gases: Atom–diatom collisions. *Phys. Fluids* **1994**, *6*, 3473–3486. [[CrossRef](#)]
14. Janssen, J.; Pitchford, L.C.; Hagelaar, G.; van Dijk, J. Evaluation of angular scattering models for electron-neutral collisions in Monte Carlo simulations. *Plasma Sources Sci. Technol.* **2016**, *25*, 055026. [[CrossRef](#)]
15. Margerin, L.; Campillo, M.; Van Tiggelen, B. Monte Carlo simulation of multiple scattering of elastic waves. *J. Geophys. Res. Solid Earth* **2000**, *105*, 7873–7892. [[CrossRef](#)]
16. Fan, J. A generalized soft-sphere model for Monte Carlo simulation. *Phys. Fluids* **2002**, *14*, 4399–4405. [[CrossRef](#)]
17. Nikolakopoulos, A.; Lovato, A.; Rocco, N. Relativistic effects in Green’s function Monte Carlo calculations of neutrino-nucleus scattering. *arXiv* **2023**, arXiv:2304.11772.
18. Keeler, H.P. Notes on the Poisson point process. Tech. Rep. Weierstrass Inst.: Berlin, Germany, 2016. <https://hpaulkeeler.com/wp-content/uploads/2018/08/PoissonPointProcess.pdf> (accessed on 30 September 2023).
19. Jayaraj, A.; Siloi, I.; Fornari, M.; Nardelli, M.B. Relaxation time approximations in PAOFLOW 2.0. *Sci. Rep.* **2022**, *12*, 4993. [[CrossRef](#)] [[PubMed](#)]
20. Wolfson, I.; Schramm, N.R.; Biton, Y.Y.; Ben-Abu, Y. The rain stick, a simple model for the dynamics of particles passing obstacles in a gravitational field. *Phys. A Stat. Mech. Appl.* **2019**, *528*, 121473. [[CrossRef](#)]

Disclaimer/Publisher’s Note: The statements, opinions and data contained in all publications are solely those of the individual author(s) and contributor(s) and not of MDPI and/or the editor(s). MDPI and/or the editor(s) disclaim responsibility for any injury to people or property resulting from any ideas, methods, instructions or products referred to in the content.